

general agreement yet according to (Akbari 2013, 2014). In this research, the following coefficients proposed by Irmay (1958) are employed in our formulation.

$$a(\varepsilon) = \alpha_c \frac{v_w (1 - \varepsilon)^2}{\varepsilon^3 D_{50}^2} : \text{Linear coefficient} \quad (5)$$

$$b(\varepsilon) = \beta_c \frac{(1 - \varepsilon)}{\varepsilon^3 D_{50}} : \text{Non-linear coefficient} \quad (6)$$

D_{50} in above equations represents the average diameter of the medium. There are also many proposals for the linear porous parameter α_c and the non-linear porous parameter β_c in Eq. (5) and Eq. (6). By referring to (Akbari 2013, 2014), α_c and β_c are set to 100 and 1.1 in this study.

3. The formulation of a stabilized ISPH method

A stabilized ISPH method, formulated by Asai (2012), is one of the particle methods for incompressible fluid. The characteristic point of this method is the relaxation coefficient which plays an key role to introduce the effect of the density-invariance condition into the general Pressure Poisson Equation. In this section, the stabilized ISPH method reformulated based on the unified governing equations will be summarized. (For details see Morimoto 2014.)

3.1 The basic concept of SPH method

Here, the fundamental concept of the scheme will be summarized. A physical scalar function $\phi(x, t)$ at an arbitral sampling point x may be approximated as

$$\phi(x, t) \approx \int_V W(|x - y|, h) \phi(y, t) dy \quad (7)$$

where W is called as the smoothing kernel function. In this research, the cubic B-spline curve proposed by Monaghan (1985) is adopted. For the SPH numerical analysis, the integral equation (7) is rewritten using the summation notation, considering the contribution of neighbor-discretized particles in the range of the smoothing length h .

$$\langle \phi_i \rangle (\approx \phi(x_i, t)) := \sum_j \frac{m_j}{\rho_j} W(r_{ij}, h) \phi(x_j, t) \quad (8)$$

Here, the subscripts i and j indicate the particle numbers, while ρ_j and m_j are the representative density and the representative mass related to the particle j respectively. The triangle blankets $\langle \bullet \rangle$ indicate the SPH interpolation calculated by referring to the neighbor particles inside the supported domain.

3.2 Pressure Poisson Equation considering seepage flow

Assuming that slight compressibility is allowed; the density-invariance condition is not needed to be satisfied instantaneously, while considerably smaller incremental particle density than the actual density difference may be given by multiplying the coefficient, α .

$$\langle \Delta \bar{\rho}_i^n \rangle \approx \alpha (\bar{\rho}_i - \langle \bar{\rho}_i^n \rangle) \quad (9)$$

Here, α ($0 \leq \alpha \leq 1$) is called as the relaxation coefficient, and is set to 0.01 in this research. Then, the Pressure Poisson Equation may be described as

$$\langle \nabla^2 P_i^{n+1} \rangle \approx \frac{C_r(\varepsilon_i)}{\varepsilon_i} \left(\frac{\bar{\rho}_i}{\Delta t} \langle \nabla \cdot \mathbf{v}_{Di}^* \rangle + \alpha \varepsilon_i \frac{\bar{\rho}_i - \langle \bar{\rho}_i^n \rangle}{\Delta t^2} \right) \quad (10)$$

According to the above formulation, good distribution in pressure is obtained by referring to the velocity distribution in each time step. Furthermore, the error related to density may be eliminated gradually by the effect of the density-deference term. Since density is almost kept constant during the numerical computation, this analysis scheme can also yield fairly good conservation of volume.

4. The physical quantity of a mound particle

In this research, the following three physical quantities related to a mound particle, which are the piezo water head, hydraulic gradient and coefficient of permeability, need to be evaluated. Note that the mound particles are not related to the SPH computation, and just handled as reference points for observing physical quantities. These physical quantities are calculated on water particles first. Then, these obtained physical quantities are interpolated into a mound marker following the SPH approximation. Moreover, the threshold for piping destruction is also introduced.

4.1 The physical quantities for a mound

The piezo water head is given according to its definition as

$$Piezo_i = \frac{P_i}{\rho_i^w \mathbf{g}_i} + \Delta z_i \quad (11)$$

where, Δz is the height from the settled datum. Note that the density is defined as ρ^w on the first term in the right hand side of Eq. (11). Moreover, the hydraulic gradient is defined as the gradient of the piezo water head as follow:

$$\mathbf{i}_i = \langle \nabla Piezo_i \rangle = \hat{\rho}_i \sum_j m_j \left(\frac{Piezo_j}{\hat{\rho}_j^2} + \frac{Piezo_i}{\hat{\rho}_i^2} \right) \nabla W(r_{ij}, h) \quad (12)$$

The coefficient of permeability is given by

$$\mathbf{k}_i = \frac{\mathbf{v}_i}{\mathbf{i}_i} \quad (13)$$

All these three physical quantities are related to water particle. Then, the physical quantity on the mound marker ϕ_i^{mound} is estimated by referring to the physical quantity on water particle ϕ_j^{water} using the weighting function.

$$\phi_i^{mound} = \sum_{j \in \text{water}} \phi_j^{water} W(r_{ij}, h) \frac{m_j}{\rho_j} \quad (14)$$

4.2 The threshold for judging piping destruction

For judging piping destruction, the hydraulic gradient on the mound marker, which is given by interpolating the hydraulic gradient of water particle into the mound marker using the SPH approximating function Eq. (14), is compared with the critical hydraulic gradient proposed by Terzaghi (1948).

The critical hydraulic gradient is defined as

$$i_c = \frac{\gamma'}{\gamma_w} = \frac{G_s - 1}{1 + e} \quad (15)$$

where, γ_w and γ' are the unit weight of water and the submerged unit weight of the soil respectively. G_s is the specific gravity of the mound particle, and is set to 2.03 referring to the experiment conducted by Kasama (2013). e is the void ratio, which is defined as $e = \varepsilon / (1 - \varepsilon)$. As a fundamental study, the condition of the mound marker is considered to change from the fixed-condition to the moveable-condition when the norm of the gradient of the piezo water head on the mound marker exceeds the critical hydraulic gradient defined by Eq. (15).

5. Numerical test

As an objective of this numerical test, the hydraulic experiment conducted by Kasama (2013) is selected. In this section, the analysis model and results will be described.

5.1 The experimental model and analysis model

The experimental model is shown in Fig.1. The water level of both outside and inside a port was being kept at the same level during the experiment by the effect of the installed drainage function. There are 25 water-pressure gauges to measure the piezo water head. In the experiment, the four different cases in water-level difference Δh , 40mm, 80mm, 120mm and 145mm, were conducted. In particular, piping destruction was observed when the water-level difference is 145mm. Therefore, only one case with $\Delta h = 145\text{mm}$ is only taken into consideration in this study.

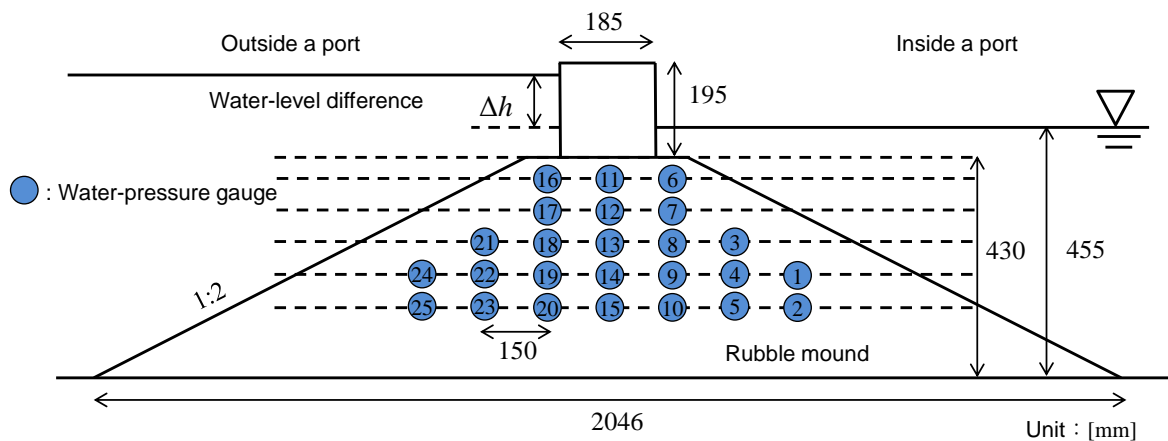


Fig.1 Experimental model

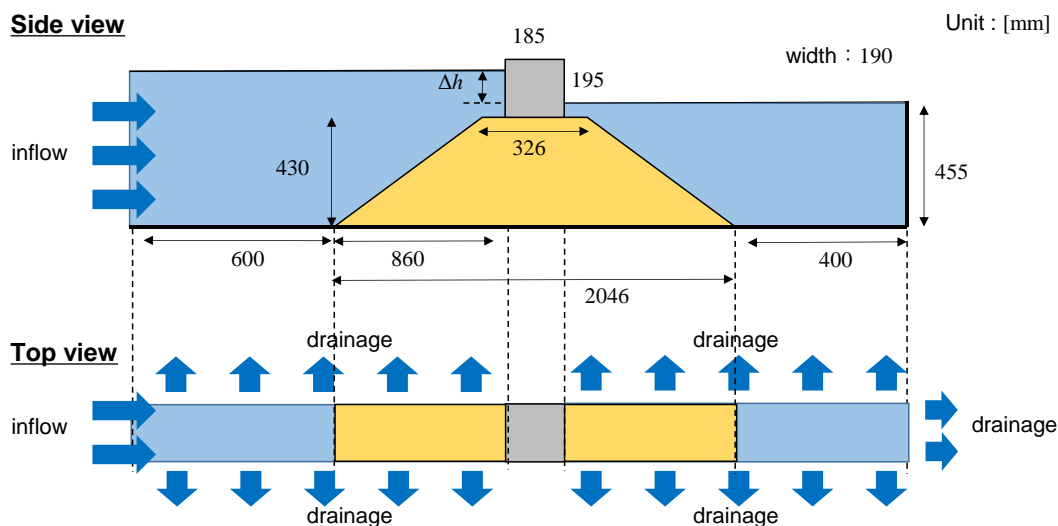


Fig.2 Analysis model

Meanwhile, the analysis model is presented in Fig.2. For the analysis model, 25 reference points are also provided at the same locations as the experimental model and the measured piezo water in numerical analysis will be compared with the experimental result. The total number of particles is approximately 900 thousand, as well as the diameter of particles is set to 1cm. The time increment is 0.001sec.

5.2 Analysis result of the distribution in piezo water head

Fig.3 shows the distribution in piezo water head when the seepage flow inside the mound is almost steady. The datum, for calculating piezo water head using Eq. (11), is set to the same height as the water level inside the port by referring to the experiment. Note that the distribution in piezo water head in Fig.3 is the interpolated distribution on the mound markers. Fig.4 illustrates the measured piezo water head at 25 water-pressure gauges. As can be seen in fig.4, there are slight difference in piezo water head between the experimental and analytical results. This error may be considered to be caused from the difficulty to keep the water at the settled level in both experiment and analysis.

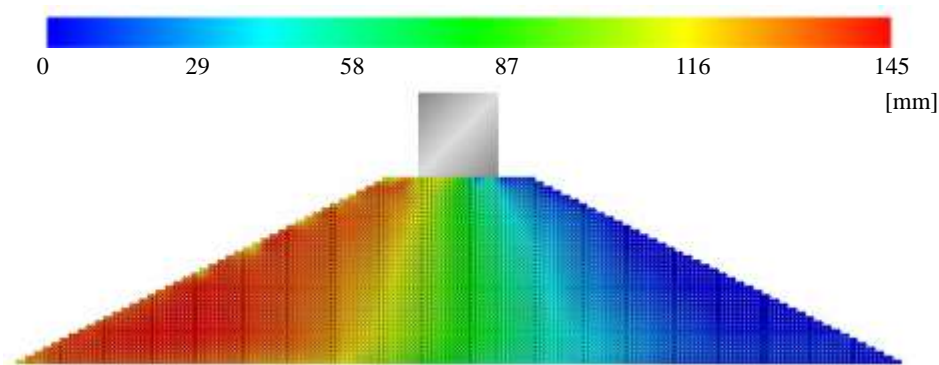


Fig.3 Distribution in piezo water head

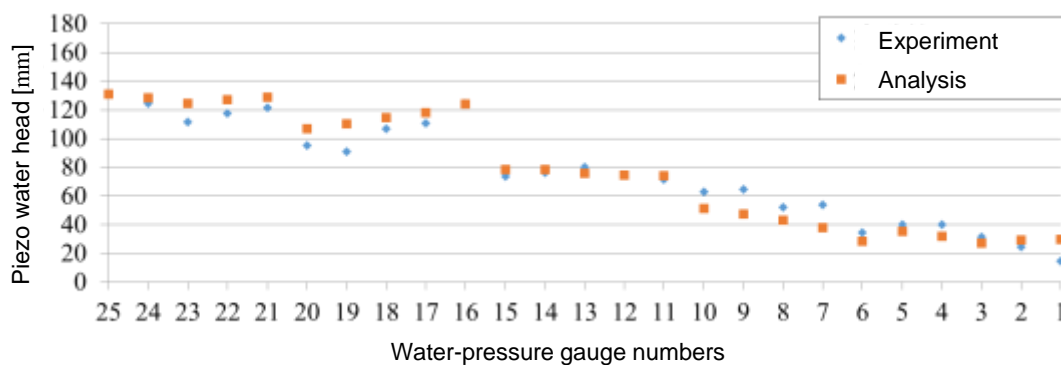


Fig.4 Measured piezo water head at the 25 water-pressure gauges

5.3 Analysis result of piping destruction

Fig.5 depicts the result on the projection of piping destruction using the critical hydraulic gradient. Note that the movement of the caisson is not taken into consideration in this study. As shown in Fig.5, it is confirmed that piping destruction starts up in the rear of the mound and under the caisson, as well as the shape of piping destruction was reproduced qualitatively. However, the development of piping phenomenon in this analysis is considerably faster than the experiment. The reasons may be as follows; (i) the caisson does not play a role to suppress the mound due to no contact force considered between the caisson and mound particles. (ii) the movable mound particle is not handled in a proper way, particularly in its motion. (iii) the contact between mound particles is not taken into account in this study.

6. Conclusion

In this research, it is confirmed that good distribution in piezo water head, which corresponds quantitatively to the experiment implemented by Kasama (2013), was obtained by using a stabilized ISPH method based on the unified governing equations. Moreover, the shape of piping destruction of the mound is reproduced qualitatively, though there are still some required modifications to be done.

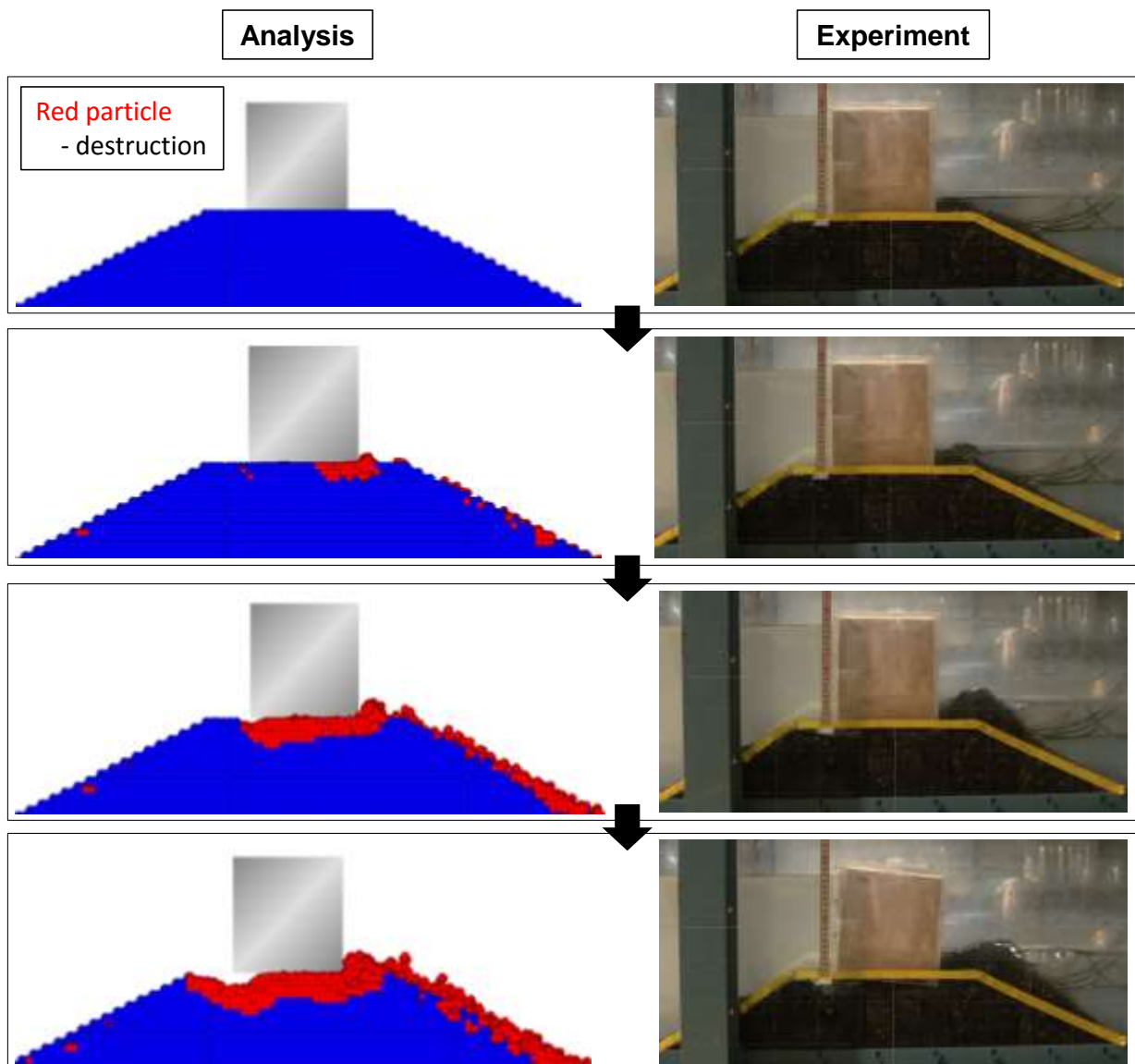


Fig.5 Projection of piping destruction

ACCKNOWLEDGEMENT

This work was supported by JSPS KAKENHI Grant Numbers 15K12484 and 26282106. This work was also partially supported by the "Advanced Computational Scientific Program" of the Research Institute for Information Technology, Kyushu University and "Joint Usage/Research Center for Interdisciplinary Large-scale Information Infrastructures(Project ID:jh160048)" in Japan.

REFERENCES

- Akbari, H. (2013), "Moving particle method for modeling wave interaction with porous structures", *Coastal Engineering* 74, pp59-73.
- Akbari, H. (2014), "Modified moving particle method for modeling wave interaction with multi layered porous structures", *Coastal Engineering* ., 89, 1-19.
- Asai, M., Aly, M.A., Sonoda, Y. and Sakai, Y. (2012), "A Stabilized Incompressible SPH Method by Relaxing the Density Invariance Condition", *Journal of Applied Mathematics.*, Volume 2012, Article ID 139583, 24pages.
- Irmay, S. (1958), "On the theoretical derivation of Darcy and Forchheimer formula", *Am. Geophys. Union* 39, 702-707.
- Kasama, K., Zen, K. and Kasugai, Y. (2013), "Model experiment for the instability of caisson-type composite breakwater under tsunami condition", *Proceeding of Coastal engineering, JSCE*, 2013.
- Monaghan, J.J. and Lattanzio, J.C. (1985), "A refined particle method for astrophysical problems", *Astronomy and Astrophysics*, Vol.149, No.1, p135-143.
- Morimoto, T., Asai, M., Kasama, K., Fujisawa, K. and Imoto, Y. (2014), "Unified numerical analysis between the extended Darcy's law and Navier-Stokes Equation by using stabilized ISPH method", *Journal of Japan Society of Civil Engineers, Ser. A2 (Applied Mechanics)*, Vol.70, pp. I_213-I_221.
- Terzaghi, K. and Peck, R.B. (1948) "Soil mechanics in engineering practice", New York, John wiley & sons, inc., London, Chapman & Hall, Ltd.
- Van Gent, M.R.A. (1995), "Wave interaction with permeable costal structures", Delft University of Technology, Delft, The Netherlands